



Smart optical CMOS sensor for endoluminal applications

Monica Vatteroni^{a,*}, Daniele Covi^b, Carmela Cavallotti^a, Luca Clementel^b,
Pietro Valdastrì^a, Arianna Menciassi^a, Paolo Dario^a, Alvise Sartori^b

^a CRIM Lab, Scuola Superiore Sant'Anna, via Piaggio, 34, 56025 Pontedera, Pisa 56100, Italy

^b NEURICAM s.r.l., Trento 38100, Italy

ARTICLE INFO

Article history:

Received 30 September 2009

Received in revised form 22 March 2010

Accepted 23 March 2010

Available online 4 April 2010

Keywords:

Biomedical

Imaging

Sensor

CMOS

ABSTRACT

A custom CMOS image sensor designed for low power endoluminal applications is presented. The fabricated chip includes a 320×240 pixel array, a complete read-out channel, a 10-bit ADC converter, a series of DACs for internal references and digital blocks for chip control. The complete functionality of the chip is guaranteed through 7 signal pins, used for the I²C-like input and LVDS output interfaces. Prototypes were produced using UMC 0.18 μm -CIS (CMOS Image Sensor) technology for both monochrome and colour-RGB versions. Due to its high sensitivity, a pinned photodiode was implemented. The imager was electrically and optically characterized and preliminary *ex-vivo* tests were performed. Characterization results show state-of-the-art performance in terms of power consumption (<40 mW for the core), which is less than half compared to off-the-shelf sensors, and light sensitivity (0.1 lux@555 nm for the monochrome imager), which makes sensor performance comparable to CCD technology performance for single chip endoluminal applications.

© 2010 Elsevier B.V. All rights reserved.

1. Introduction

The continuous quest for painless diagnostic procedures in the gastro-intestinal tract has resulted in greater interest in endoluminal techniques, such as capsular endoscopy [1]. An endoscopic capsule is a swallowable self-contained microsystem which performs a sensing or actuating function in the body [2]. The swallowable capsule concept first appeared in 1957 in Mackay and Jacobson's paper on RF transmission of pressure and temperature from the human body [3]. Although the concept of capsule endoscopy emerged as an alternative to traditional endoscopy during the 80s and 90s, the first capsule endoscope model was developed by Given Imaging in 2000 [4] and received medical approval in Western countries in 2001. The first capsule was commercialized by Given Imaging with the name of PillCamTMSB, especially designed for small bowel investigation. Essentially, the PillCamTMSB is a swallowable wireless miniaturized camera which provides images. Despite research on actuation [5], drug delivery and biopsy techniques that may be implemented in an endoscopic capsule [2,6,7], the imaging unit is still the core part of the system. The main goal of endoscopy is to inspect the inside of the body through imaging techniques for diagnostic and surgical purposes. For this reason, image quality is a primary issue in both traditional and innovative endoscopic devices.

Given Imaging is a major worldwide industrial player in the field of capsular endoscopy and commercializes solutions for different gastro-intestinal tracts: the PillCamTMSB, PillCamTM ESO and PillCamTMCOLON. All these pills implement a complementary metal oxide semiconductor (CMOS) imager acting as sensor, but they present different frame rate characteristics. Alternative endoscopic pills to those commercialized by Given Imaging are the EndoCapsule created by Olympus [8], the MiroCamTM by IMC [9], and OMOM by Jinshan Science & Technology Company [10]. Although CMOS is the most common technology, the EndoCapsule integrates a Charge Couple Device (CCD). Resolution of these systems ranges between 256×256 and 1000×1000 pixels, while the frame rate ranges between 2 and 7 frames per second (fps). The basic trade-off for a vision system for capsular endoscopy is to be found between high image quality and other features such as size, power consumption, simple control interfaces, image resolution and frame rate. Off-the-shelf chips can only partially fulfil these requirements. Some sensors provide good image resolution and quality in a small size, but lack adequate sensitivity and acceptable power consumption [11]. Other imagers feature low power requirements and small size, but still present poor output in terms of noise and image quality [12]. Novel sensors have appeared on the market over the last few months featuring low power consumption, good image quality and small size [13]. However, their analogue output makes them unsuitable for capsular endoscopy because a companion chip is needed for converting the analogue output into digital word. This results in an increase in space and power consumption. For this reason, the highly specific and demanding requirements of capsular endoscopy

* Corresponding author. Tel.: +39 050883483; fax: +39 050883496.

E-mail address: m.vatteroni@sssup.it (M. Vatteroni).

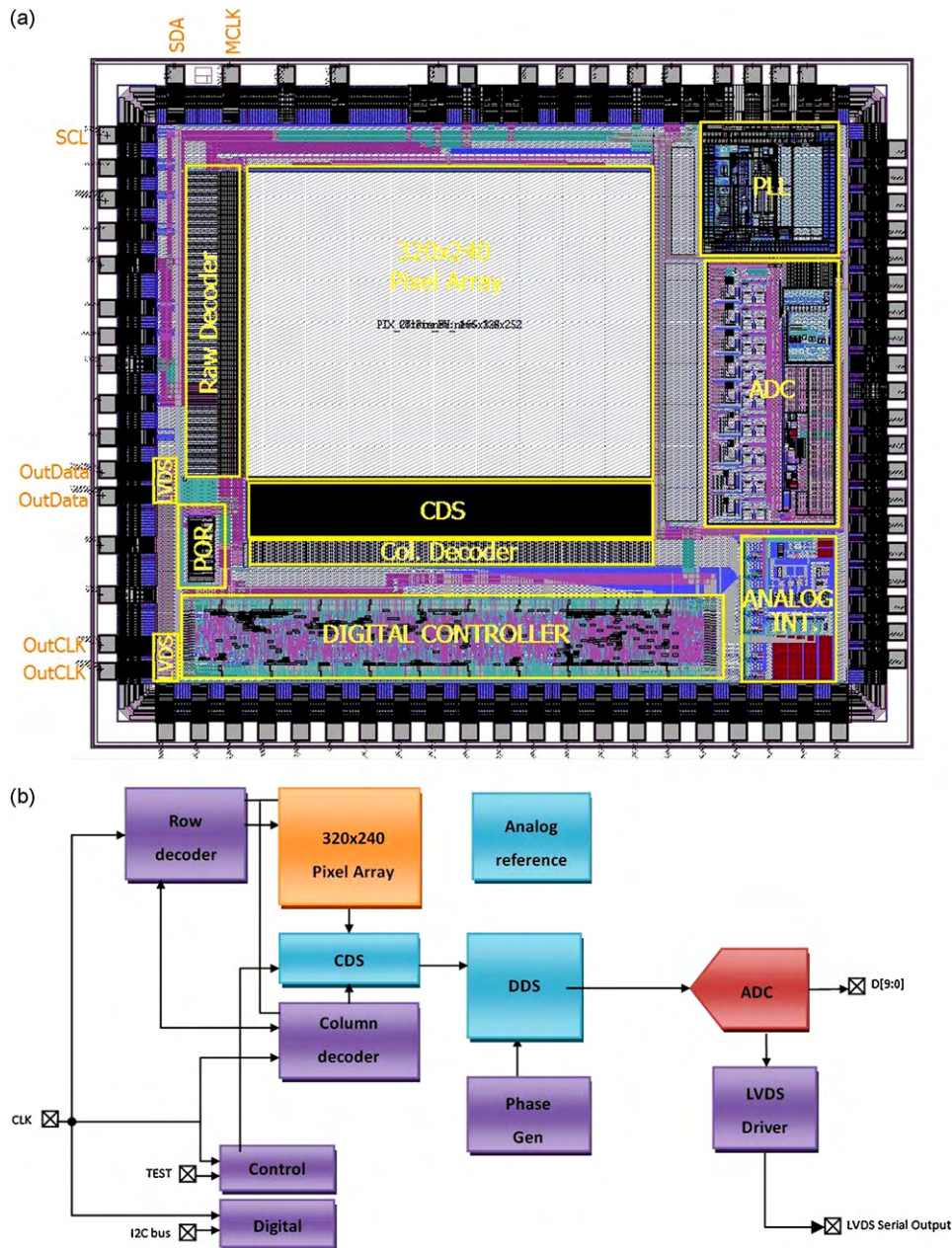


Fig. 1. Layout of the Vector2 sensor (a). Block diagram of the Vector2 chip (b).

have motivated the development of a novel image sensor. CMOS technology was chosen for single chip endoluminal applications because it is simpler to control and consumes less power than CCD technology [14]. The imager presented in this paper, called Vector2, was designed to improve sensitivity and at the same time reduce power consumption, by using a simple control interface requiring a few pins. The main features targeted during the design phase were high sensitivity [15,16], low power consumption and a simple control interface through a reduced number of pins. A resolution of 320×240 pixels was considered to be a good compromise between image quality, chip dimensions and frame rate, in terms of telemetry payload. All the internal blocks were designed to guarantee low power consumption and easy chip control. The circuitry integrated in the chip comprises the analogue and digital blocks needed for full automatic control of the sensor core through a 2-pin I²C-like input interface and a 4-pin low-voltage differential signaling (LVDS) output interface. Prototypes were fabricated using the UMC 0.18 μm -CIS technology and characterized in both monochrome

and colour versions. In order to exhaustively describe the presented device, the imager architecture is presented in Section 2, while performance of the device is presented in Sections 3 and 4 together with the results of the electro-optical characterization and *ex-vivo* tests.

2. Imager architecture and operation of the camera

Vector2 is a monolithic 320×240 active-pixel colour-RGB or monochrome camera-on-a-chip sensor. The chip is fabricated with UMC 0.18 μm CMOS technology which is optimized for optical applications. This process was chosen because it allows the use of pinned photodiode technology, implemented in the UMC ultra-photodiode pixel [17]. A pinned photodiode has the same structure as an active-pixel with the addition of an extra photodiode, which is pinned by depositing a p-plus doped thin silicon layer. This additional junction is connected to the read-out circuit by means of an

Table 1
Vector2 imager main characteristics.

| Main characteristics | Dimension | Value |
|----------------------|-----------------|-----------|
| Resolution | | QVGA |
| Active area | | 320 × 240 |
| Optical format | Inch | 1/9 |
| Pixel pitch | μm^2 | 4.4 × 4.4 |
| Fill factor | % | 25 |
| Shutter type | | Rolling |
| Die size | mm^2 | 2.5 × 3.0 |

extra transfer gate which ensures separation of the sensing junction from the read-out node. The pinned structure of the photosensitive element shields it from the Si – SiO₂ interface, which is a source of noise and leakage, reducing the dark current and enhancing sensitivity. Furthermore, the additional junction, due to the extra layer, increases intrinsic charge storage capacitance [18]. This technology was mainly selected because of the possibility to reach high levels of sensitivity [19], which is one of the main specifications to be achieved. The sensor architecture is outlined in Fig. 1. The sensor operates in conjunction with a host microcomputer or microcontroller. They are connected through a serial LVDS output, which carries the video data to the processor. The serial output has the advantage of high speed transmission through a small number of pins, as outlined in the specifications above. As regards data protocol, the mobile industry processor interface (MIPI) standard [20] was considered. A simplified version of this protocol was used in order to reduce the number of external connections and control lines. An I²C-like interface was implemented for the low rate input control and setting of the chip. The I²C-like interface was selected because it is well established, simple to use and suitable for this application. Therefore, the number of pins used in normal operation is limited to 7 for simple chip control, as required by applications which need a small number of connections. A number of test pins are also available to guarantee a high level of flexibility and the possibility to shift control complexity to external logic. The imager integrates a pixel array based on the UMC ultra-photodiode technology [21]. However, it was decided that pixel driving should have a rolling shutter read-out in order to maximize sensitivity of the sensor.

The main characteristics of the imager are reported in Table 1. Pixel pitch is 4.4 μm and fill factor is 25%, due to control and read-out transistors integrated in the pixel. The optical format with quarter video graphics array (QVGA) resolution results in 1/9 of inch. As evident from Fig. 1(a), total die size is dominated by the pixel array. Due to the other required conditioning and control blocks, final chip dimension is 2.5 × 3.0 mm^2 .

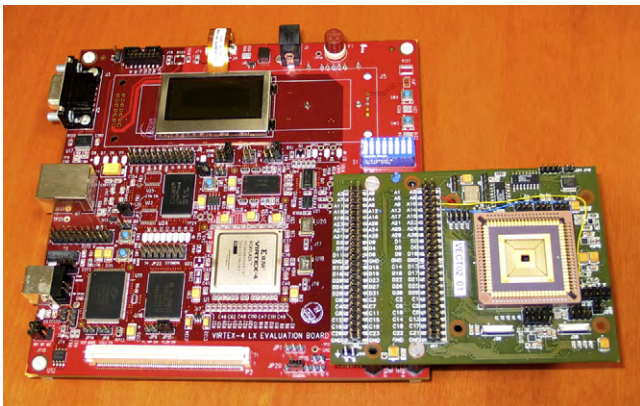


Fig. 2. Vector2 test development board.

The primary goal of the design was to obtain high quality images. Therefore, to achieve this result, it is important to minimize system noise. Sources of noise in a CMOS imager are both optical and electrical. Optical noise can be reduced with an optimized layout of the pixel and with a protective shield covering the remaining circuitry. The shield can be made of metal layers or achieved by post processing coating. The latter technique was used for Vector2 since available in the standard chipset processing masks by UMC. Electrical noise contribution can be classified as spatial noise, called Fixed Pattern Noise (FPN) due to process mismatch, and temporal noise, called Pixel temporal Noise (PN). FPN is less critical and can be reduced by one or more signal filtering steps. This operation is carried out in Vector2, at column level, by a column data sampling (CDS) block which performs a first signal subtraction to reduce the pixel FPN. A second subtraction is then performed, this time at array level, by a data double sampling (DDS) block, which subtracts the FPN introduced by the mismatch between the different CDS blocks. PN is minimized by designing a read-out channel with techniques dedicated to obtaining low-noise, i.e. special layout adjustments and fully differential blocks were used wherever possible.

The read-out is completed by converting the analogue signal into a digital signal by means of a pipeline ADC architecture [22]. This converter architecture was chosen since it represents a good compromise between speed, power consumption and output linearity required by the application. Considering a noise level below 1 mV and a full signal range of 1 V, 10-bit resolution was considered adequate for our purposes.

Due to a strict constraint on the number of external connections, the required voltage references were generated internally by means of digital to analogue converters (DAC) integrated onto the chip. The architecture is completed with row and column decoders for single pixel selection and custom digital blocks for sensor core and interface control.

The read-out of the analogue pixel outputs starts with the selection of a row, by means of a row decoder. Pixel FPN and low frequency noise are filtered, line by line, carrying the signal, V_{SigPix} , and the reset value, V_{ResPix} , to the CDS amplifiers [23]. CDS output, $V_{\text{ResCDSout}}$ is proportional to these signals as:

$$V_{\text{SigCDSout}} = [V_{\text{SG}} + (V_{\text{ResPix}} - V_{\text{SigPix}}) \times G_{\text{SFpix}} + V_{\text{bCDS}}] \times G_{\text{SFCDs}} \quad (1)$$

The buffer gain of the pixel and CDS, G_{SFpix} and G_{SFCDs} respectively, and the threshold V_{SG} are technology- and layout- dependent due to the possible mismatch between different transistors. The signal V_{bCDS} is a reference set by the user to avoid direct ground connection and to allow a controlled shift of the output signal.

The CDS outputs are then sequentially selected one at a time by means of the column decoder, and further filtered in series by the DDS block to remove the column FPN [24]. A CDS reference value, $V_{\text{ResCDSout}}$, is obtained by setting the CDS in the reset configuration and is used for this filtering.

$$V_{\text{ResCDSout}} = [V_{\text{SG}} + V_{\text{bCDS}}] \times G_{\text{SFCDs}} \quad (2)$$

The DDS block is a fully-differential switched capacitor block which provides a differential output, V_{OutDDS} . These signals are proportional to the signal and reset outputs of the CDS read-out by a gain

Table 2
Vector2 imager electrical characteristics.

| Main characteristics | Dimension | Value |
|-----------------------|-----------|-----------------------|
| Master clock | MHz | 25 |
| Data rate | MHz | 100 |
| Pixel rate | MHz | 10 |
| Data format | Bit | 10-serial |
| Power consumption | mW | < 40 (@30 fps, 27 °C) |
| Operating temperature | C | -40/ + 80 |

Table 3
Vector2 optical performance.

| Parameter | Unit | Monochrome | Colour-RGB |
|---------------------------|--------------------------------------|--|--|
| Sensitivity | lux W/m ² | 0.11@555 nm, 27 °C, 30 ms 1.70 × 10 ⁻⁴ , @27 °C, 30 ms | 0.32@555 nm, 27 °C, 30 ms 4.65 × 10 ⁻⁴ @27 °C, 30 ms |
| Responsivity | V/lux*se °C V/W/m ² *s | 0.53@555 nm, 27 °C 360@27 °C | 0.12@555 nm, 27 °C 81@27 °C |
| Dynamic range | dB | 50 | 60 |
| SNR | dB | 46 (max) | 53 (max) |
| Pixel Temporal Noise(PN) | % | 0.70 | 0.25 |
| Fixed Pattern Noise (FPN) | % | 0.86 | 1.67 |

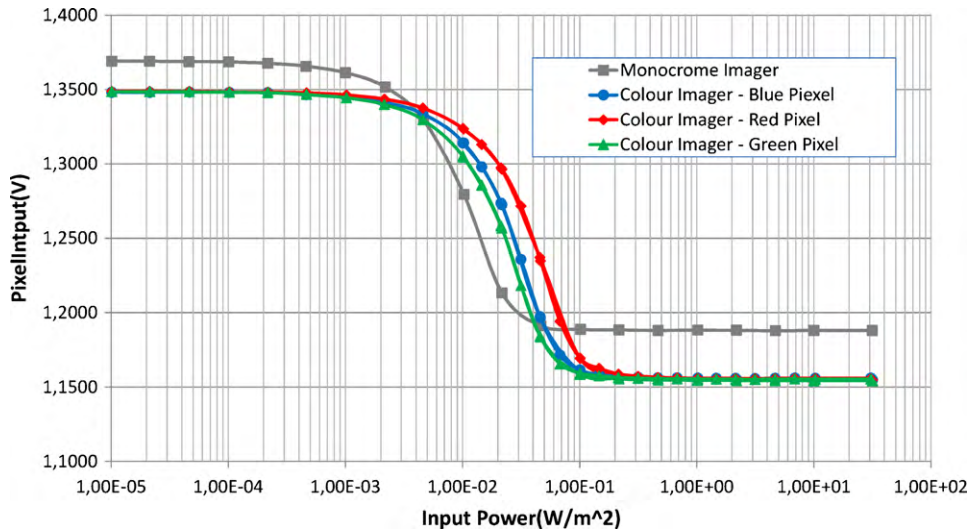


Fig. 3. Vector2 power responsivity as function of irradiation power for the black and white sensor and the colour-RGB sensor in the three different colours.

factor, G_{DDS} , but also to a common mode signal, V_{CM} .

$$V_{OutDDS} = V_{CM} \pm G_{DDS} \times (V_{REF} - (V_{ResCDSOut} - V_{SigCDSOut})) \quad (3)$$

The G_{DDS} gain is incorporated in the DDS block, programmable by the user and set via I²C. The gain is set by changing the ratio between switched capacitances. Available gain values are between 0 and 8 with a precision of 256 steps.

Finally, the DDS output is converted into a digital word, ADCOUT, by the on-chip 10-bit pipeline ADC and then serialized.

$$ADCOUT = \frac{(V_{OutDDS}^+ - V_{OutDDS}^-)}{(V_{REFP} - V_{REFN})} \times 2^9 \quad (4)$$

The voltage range accepted at the ADC input is defined by two reference voltages, V_{REFP} and V_{REFN} , with typical values of 1.5 V and 0.3 V respectively.

All the described functions are related to the analogue core of the imager.

3. Imager characterization

A test board was designed and developed to characterize the Vector2 chip (Fig. 2). The set-up is composed of a main board and a dedicated 'eye PCB' designed for specific chip control. This set-

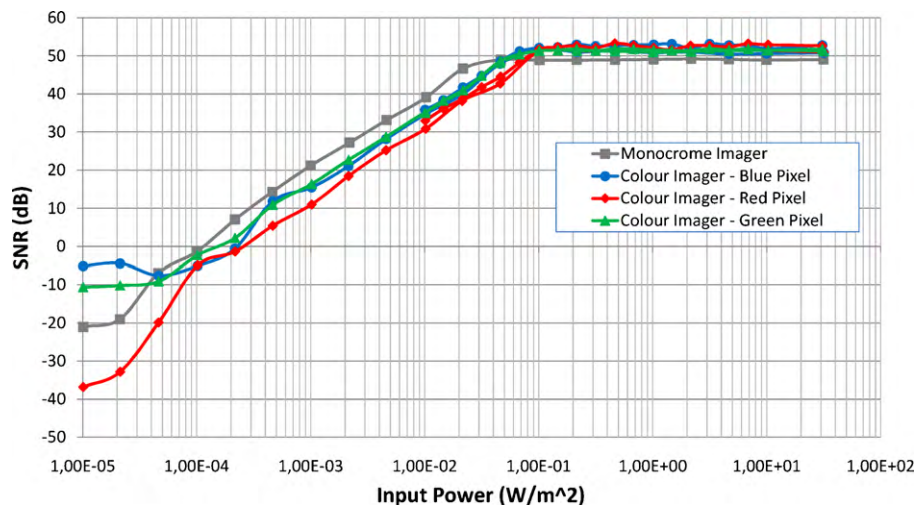


Fig. 4. Vector2 SNR as function of irradiation power for the black and white sensor and the colour-RGB sensor in the three different colours.

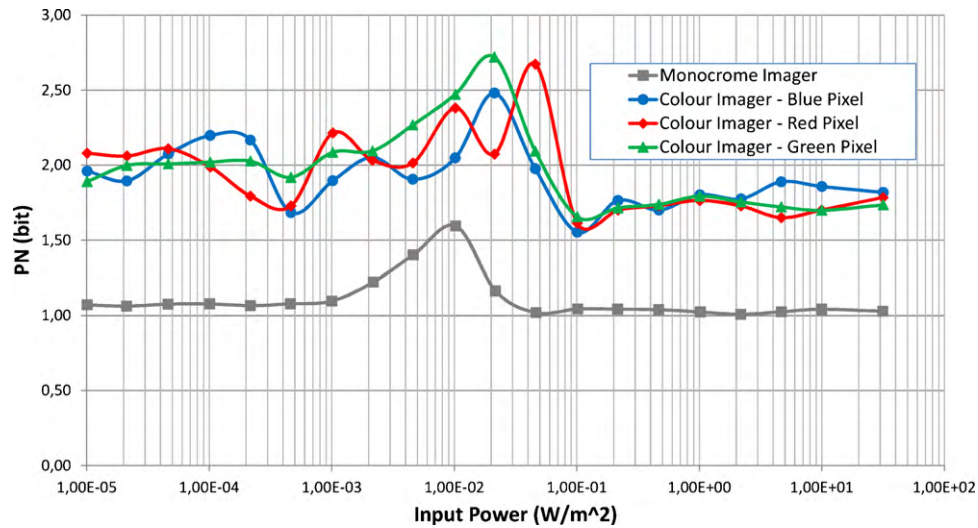


Fig. 5. Vector2 PN as function of irradiation power for the black and white sensor and the colour-RGB sensor in the three different colours.

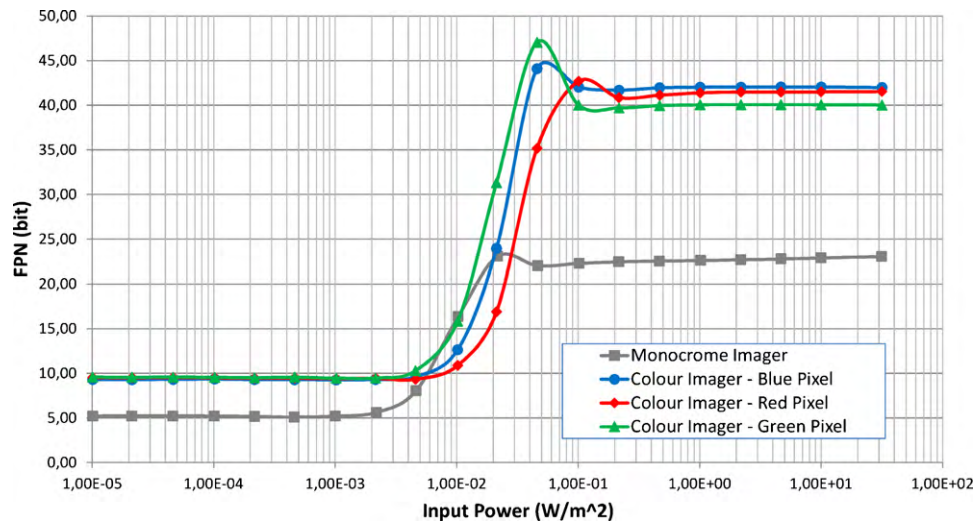


Fig. 6. Vector2 FPN as function of irradiation power for the black and white sensor and the colour-RGB sensor in the three different colours.

up was used for both electrical and optical characterization. As summarized in Table 1 the chip is supplied with voltages equal to 1.8 V and 3.3 V. Typical values for the master and output clocks are 25 MHz and 100 MHz respectively, with a duty cycle of 50% in both cases. Complete functionality of the Vector2 sensor was successfully verified using the test board. Most of the internal blocks were characterized independently, mainly to check output voltage swing and linearity of response. Power consumption during normal operation was measured as a crucial parameter, being less than 40 mW with a frame rate of 30 fps. Significant parameters, such as optical sensitivity, noise and dynamic range, were extracted through optical characterization of both the monochrome and colour-RGB sensor.

The main test results are shown in Table 2. Optical sensitivity was measured as 0.11 lux for the monochrome sensor and 0.32 lux for the colour-RGB sensor. Sensitivity was measured with an integration time of 30 ms at ambient temperature (27 °C) and with a 555 nm wavelength. Dynamic range and signal to noise ratio (SNR) are reported in Table 3 as average and maximum values, and in Figs. 3 and 4 as function of the light power for both the monochrome and the colour-RGB sensors. It is quite clear that Dynamic range and SNR performance are better for the colour-RGB sensor given the

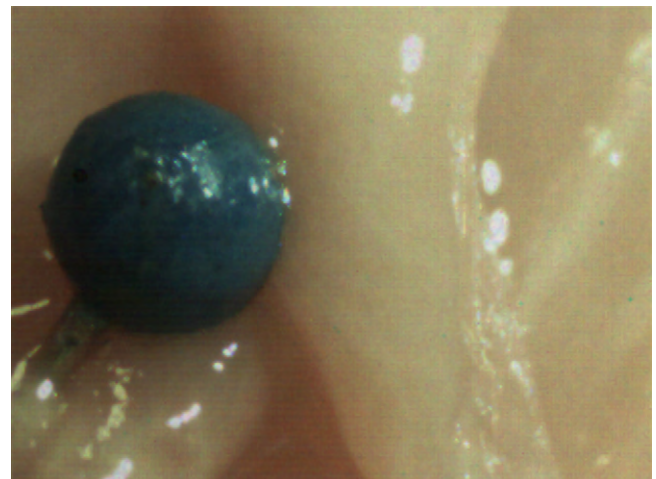


Fig. 7. Example of *ex-vivo* image acquired with the Vector2 optical sensor.

lower responsivity. Noise numbers are also reported as a percentage of the average value over the full signal range and as a function of illumination power (Figs. 5 and 6). PN [25], consisting of temporal noise, is higher for the monochrome sensor (0.70%), but still lower than the level perceived by the human eye, which is over 5% [26]. FPN, which represents spatial noise, is double in the colour-RGB version (1.67%) compared to the monochromatic version (0.86%).

4. Ex-vivo tests

When working with an endoscopic camera, it is necessary to consider the non-standard settings required by the camera to capture important biological information in the image, which differ from many other types of imaging systems. For this reason it is important to perform tests on biological tissues, to evaluate image quality and to set the sensor accordingly. In particular, colour gain can be adjusted in order to receive the best response.

Ex-vivo images were acquired with the colour-RGB version of the Vector2 imager and with non-optimized optics, in order to receive preliminary indications on image quality for target application. Tests were conducted on freshly excised porcine colon tissue attached to the test bench, which also included the test board. An example of an acquired image is shown in Fig. 7. The image is obtained by applying demosaicing and background subtraction. As expected by the results obtained on noise performance, image quality is good in terms of uniformity. Original colour rendition can also be considered good and can be further improved by image processing.

Additional ex-vivo tests will be carried out to optimize the camera setting and to better understand imager performance.

5. Conclusions and future work

A CMOS image sensor specifically designed for wireless endoluminal applications was presented. As required by the application, a trade-off was identified for crucial parameters such as chip size, power consumption and image quality, and a custom design was developed to meet the required specifications. Electrical and optical characterizations demonstrated that targeted requirements in terms of power consumption and high sensitivity have been met. The monochrome sensor has a sensitivity of 0.11 lux (@555 nm and 27 °C), while colour-RGB imager sensitivity is equal to 0.32 lux (@555 nm and 27 °C). These characteristics are comparable to CCD devices for single chip endoluminal applications. Power consumption is less than 40 mW in both cases. This makes the sensor suitable for wireless endoluminal applications such as capsular endoscopy. Ex-vivo and in-vivo tissue images were preliminarily acquired, showing good image uniformity, also guaranteed by low-noise performances (PN < 0.53% and FPN < 1.67%). The Vector2 chip will be further extensively tested to achieve complete and systematic characterization, focusing on the acquisition of endoluminal images. Samples of the Vector2 imager will be integrated in a complete miniaturized wireless vision system for capsular endoscopy.

Acknowledgments

The work described in this paper was funded by the European Commission within the VECTOR FP6 European project (EU/IST-2006-033970). We would like to thank Stephane Chamot and Jerome Parent from the Microvision & Microdiagnostics Group at EPFL (Ecole Polytechnique Federale de Lausanne) for their valuable support and work during the optical characterization phase.

References

- [1] R. Eliakim, Video capsule endoscopy of the small bowel, *Curr. Opin. Gastroenterol.* 24 (2) (2008) 159–166.

- [2] C. McCaffrey, O. Chevalerias, C. Mathuna, K. Twomey, Swallowable-capsule technology, *IEEE.M.PVC* 7 (1) (2008) 23–29.
- [3] R. Mackay, B. Jacobson, Endoradiosonde, *Nature* 179 (4572) (1957) 1239–1240.
- [4] G. Iddan, G. Meron, A. Glukhovsky, P. Swain, Wireless capsule endoscopy, *Nature* (2000) 405–417.
- [5] P. Valdastrì, R. Webster, C. Quaglia, M. Quirini, A. Menciassi, P. Dario, A new mechanism for mesoscale legged locomotion in compliant tubular environments, *IEEE.J.RO* 25 (4) (2009) 1–11.
- [6] A. Moglia, A. Menciassi, P. Dario, A. Cuschieri, Capsule endoscopy: progress update and challenges ahead, *Nat. Rev. Gastroenterol. Hepatol.* 6 (2009) 353–361.
- [7] T. Nakamura, A. Terano, Capsule endoscopy: past, present, and future, *J. Gastroenterol.* 43 (2) (2008) 93–99.
- [8] C. Gheorghe, R. Iacob, I. Bancila, Olympus capsule endoscopy for small bowel examination, *J. Gastrointest. Liver Dis.* 16 (2007) 309–313.
- [9] S. Bang, J.Y. Park, S. Jeong, Y.H. Kim, H.B. Shim, T.S. Kim, D.H. Lee, S.Y. Song, First clinical trial of the miro capsule endoscope by using a novel transmission technology: electric-field propagation, *Gastrointest. Endosc.*
- [10] A. Uehara, K. Hoshina, Capsule endoscope norika system, *Minim. Invas. Ther. Allied Technol.* 12 (5) (2003) 227–234.
- [11] http://www.aptna.com/products/image_sensors/mt9v013d00stcp/#overview.
- [12] http://www.ovt.com/products/part_detail.php?id=78.
- [13] http://www.ovt.com/products/part_detail.php?id=55.
- [14] D.R. Cave, D.E. Fleischer, J.A. Leighton, D.O. Faigel, R.I. Heigh, V.K. Sharma, C.J. Gostout, E. Rajan, K. Mergener, A. Foley, M. Lee, K. Bhattacharya, A multicenter randomized comparison of the endocapsule and the pillcam sb, *Gastrointest. Endosc.* 68 (3) (2008) 487–494.
- [15] O. Yadid-Pecht, B. Mansoorian, E.R. Fossum, B.P. Pain, Optimization of noise in cmos active pixel sensors for detection of ultra low light levels, *Proc. Spie* 3019 (1997) 125.
- [16] X.C. Liu, B. Fowler, H. Do, S. Mims, D. Laxson, B. Frymire, High performance cmos image sensor for low light imaging, in: *International Image Sensor Workshop*, Ogunquit, Maine, USA, 2007, pp. 327–330.
- [17] 0.18 μm cmos image sensor umc ultra photodiode process cell rule, G-1C-CMOS.SENSOR 18-UMC/ ULTRA_PD-CELL Ver. B.D.P-B, UMC foundry, 2007.
- [18] A. Theuwissen, Cmos image sensors: State-of-the-art and future perspectives, in: *Solid State Circuits Conference*, 2007. ESSCIRC 2007. 33rd European, 2007, pp. 21–27.
- [19] R. Guidash, T.-H. Lee, P. Lee, D. Sackett, C. Drowley, M. Swenson, L. Arbaugh, R. Hollstein, F. Shapiro, S. Domer, A 0.6 μm cmos pinned photodiode colour imager technology, in: *Electron Devices Meeting*, 1997, Tech. Digest., Int. (1997) 927–929, IEDM'97.
- [20] <http://www.mipi.org/>.
- [21] http://www.europpractice-ic.com/technologies_UMC.php?tech_id=018um.
- [22] S. Hamami, L.F. L. O. Yadid-Pecht, Cmos image sensor employing 3.3 v 12 bit 6.3 ms/s pipelined adc, *Sens. Actuators A* 135 (2007) 119–125.
- [23] B. Fowler, X. Liu, Charge transfer noise in image sensors, in: *2007 International Image Sensor Workshop*, Ogunquit, Maine USA, 2007, pp. 51–54.
- [24] S.K. Mendis, S.E. Kemeny, R.C. Gee, B. Pain, C.O. Staller, Q. Kim, E.R. Fossum, S. Member, Cmos active pixel image sensors for highly integrated imaging systems, *IEEE J. Solid-State Circuits* 32 (1997) 187–197.
- [25] H. Tian, B. Fowler, A.E. Gamal, Analysis of temporal noise in cmos photodiode active pixel sensors, *IEEE J. Solid-State Circuits* 1 (2001) 36.
- [26] A. Theuwissen, *Digital Imaging: Image Capturing, Image Sensors, Technologies and Applications*, CEI-Europe, 2004.

Biographies

Monica Vatteroni was born in La Spezia, Italy, in 1975. She received an M.S. degree in electrical engineering from the University of Pisa (Italy) in 2001 and a Ph.D. degree in Physics from the University of Trento (Italy), in 2008. From 2002 to 2008, she worked for NeuriCam, Trento (Italy), as Pixel Engineer and analogue designer, and in 2005 she became responsible for the development of CMOS image sensors. Presently, she works for the Scuola Superiore Sant'Anna in Pisa (Italy) as postdoctoral fellow, where she is responsible for the research and development of image sensors and vision systems for biomedical applications. She is the author and co-author of several conference and journal publications and of three patents. Her interests include CMOS image sensors, low-noise analogue electronics, high dynamic range pixels and endoscopic vision systems.

Daniele Covi graduated in physics (summa cum laude) from the university of Trento (Italy) in 2001 where he worked on the active control of magnetic fields for atomic traps. In 2005 he received an MBA from the Alma Graduate School – University of Bologna (Italy). After joining Neuricam in 2000, he took part in the design and transferred to production of CMOS optical sensors and set up the electro-optical laboratory for imaging sensors' characterization. He has been head of the VLSI Design Area since 2002. He currently works as project manager in the field of advanced electro-optical systems design. His research interests focus on optical distance measurement systems and miniaturized camera modules for endoscopy applications.

Carmela Cavallotti received a degree in biomedical engineering (with honours) from the Campus Bio-Medico University in Rome in December 2007. She is currently a Ph.D. student in biorobotics at the CRIM Lab of the Scuola Superiore Sant'Anna in Pisa.

Luca Clementel received a B.S. degree in communication engineering from the University of Trento in 2001 developing a digital neural network implemented in FPGA. He joined Neuricam Srl, Trento, in 2001, where he designed digital architectures in programmable logic devices for vision systems such as glue logic for demonstration baseboards of optical sensors and complex image processing algorithms. He is currently an HDL developer and a project manager in the field of intelligent vision systems design.

Pietro Valdastrì received a degree in electronic engineering (with honours) from the University of Pisa in February 2002. In the same year he joined the CRIM Lab of the Scuola Superiore Sant'Anna in Pisa as a PhD student. In 2006 he obtained a Ph.D. in bioengineering from the Scuola Superiore Sant'Anna discussing a thesis titled "Multi-Axial Force Sensing in Minimally Invasive Robotic Surgery". He is now assistant professor at CRIM Lab, with main research interests in the field of implantable robotic systems and active capsular endoscopy. He is currently working on several European projects for the development of minimally invasive and wireless biomedical devices.

Arianna Menciassi received a degree in physics (with honours) from the University of Pisa in 1995. In the same year, she joined the CRIM Lab of the Scuola Superiore Sant'Anna in Pisa as a Ph.D. student in bioengineering with a research programme on the micromanipulation of mechanical and biological micro objects. In 1999, she received a Ph.D. degree discussing a thesis titled "Microfabricated Grippers for Micromanipulation of Biological and Mechanical Objects". She is currently professor of biomedical robotics at the Scuola Superiore Sant'Anna, Pisa. Her main research interests are in the fields of biomedical micro- and nano-robotics, micro-fabrication technologies, micromechatronics and microsystem technologies. She is currently working on several European projects and international projects for the development of micro and nano-robotic systems for medical applications.

Paolo Dario received a degree in mechanical engineering from the University of Pisa in 1977. Currently, he is professor of biomedical robotics at the Scuola Superiore Sant'Anna, Pisa. He also set up and teaches the Mechatronics course at the School of Engineering, University of Pisa. He has been a visiting professor at the Ecole Polytechnique Federale de Lausanne (EPFL), Lausanne, Switzerland, and at Waseda University, Tokyo, Japan. He is the director of the CRIM Lab of Scuola Superiore Sant'Anna, where he supervises a team of around 70 researchers and Ph.D. students. His main research interests are in the fields of medical robotics, mechatronics and microengineering, and specifically in sensors and actuators for the above applications. He is the coordinator of many national and European projects, the editor of two books on robotics and the author of over 200 journal papers. He is a member of the Board of the International Foundation of Robotics Research. He is an associate editor of the IEEE Transactions on Robotics and Automation, a member of the Steering Committee of the Journal of Microelectromechanical Systems and a guest editor of the Special Issue on Medical Robotics of the IEEE Transactions on Robotics and Automation. He serves as president of the IEEE Robotics and Automation Society and as the co-chairman of the Technical Committee on Medical Robotics of the same society.

Alvise Sartori received an M.A. degree in Physics from the University of Oxford in 1978 and a Ph.D. in Geophysics from Imperial College, London, in 1983. He then joined the central research laboratory of Olivetti, where he carried out research on modelling of fluido-dynamic systems and design of digital CMOS integrated circuits. In 1990 he joined IRST, a Research Institute in Trento, Italy, where he was in charge of the VLSI Design Laboratory. Since 1998, he is President and CEO of NeuriCam SpA, Trento, a company he co-founded in 1998, active in the fabless production of chips and systems for computer vision.